

Bent-Crystal Spectrometer Measurement of the Intensities of X Rays Coincident with Fission of $U^{235}\dagger$

BERNARD W. WEHRING* AND MARVIN E. WYMAN

Nuclear Engineering Program, University of Illinois, Urbana, Illinois

(Received 18 January 1967)

A measurement of the intensities of K x rays from fission fragments was made using a bent-crystal spectrometer of the Johansson type. The experiment was a coincidence experiment with only those x rays in coincidence with a fission event being counted. A wire coated with enriched uranium was placed in a thermal-neutron beam and served as the fission source. This wire was both the center wire for a fission ionization chamber and the x-ray source for the bent-crystal spectrometer. In order to maintain sufficient sensitivity, resolution was sacrificed. The resolution, however, was still good enough to resolve the $K\alpha$ lines of adjacent elements of the light fragments. The experimental results for the prompt K x-ray intensities are compared with calculated initial yields versus atomic number. The apparent x-ray yield per fragment as a function of charge does not vary slowly with charge but is what one might expect for electronic vacancy production due to internal conversion by the de-exciting fragments. This effect appears to be more pronounced for thermal-neutron-induced fission of U^{235} than spontaneous fission of Cf^{252} .

I. INTRODUCTION

SINCE 1956, numerous laboratories have initiated investigations of the prompt x rays from fission.¹⁻¹¹ Since the energy of a characteristic x ray is determined by the charge of the nucleus, a measurement of the prompt x-ray spectrum could, in principle, give a direct determination of the initial charge distribution of the fission fragments. In order to gain such information, the following would need to be satisfied:

1. The experiment should be a coincidence experiment, only the prompt x rays and therefore only those from the primary fragments being counted.
2. The spectrometer should be capable of separating the characteristic x-ray lines so that x-ray intensities could be found.
3. The mechanisms for producing electronic vacancies should be understood in order that the x-ray intensities could be related to the initial charge distribution.

† The material in this article is based upon a dissertation by one of the authors (BWW) submitted in partial fulfillment of the requirements for the doctoral degree at the University of Illinois.

* Former AEC Special Fellow in Nuclear Science and Engineering sponsored by the U. S. Atomic Energy Commission. The fellowship is administered by the Oak Ridge Associated Universities.

¹ R. E. Carter, J. J. Wagner, and M. E. Wyman, *Bull. Am. Phys. Soc.* **3**, 228 (1958).

² R. B. Leachman, in *Proceedings of the Second United Nations International Conference on the Peaceful Uses of Atomic Energy, Geneva, 1958* (United Nations, Geneva, 1958), Vol. 15, p. 331.

³ V. V. Sklyarevskii, E. P. Stepanov, and B. A. Medvedev, *Zh. Eksperim. i Teor. Fiz.* **36**, 326 (1959) [English transl.: *Soviet Phys.—JETP* **9**, 225 (1959)].

⁴ F. C. Maienschein, R. W. Peelle, and T. A. Love, Atomic Energy Commission Report No. TID-6302, 1959 (unpublished).

⁵ H. Hohman, *Z. Physik* **172**, 143 (1963).

⁶ L. E. Glendenin and H. C. Griffin, *Phys. Letters* **15**, 153 (1965).

⁷ L. E. Glendenin and J. P. Unik, *Phys. Rev.* **140**, B1301 (1965).

⁸ S. S. Kapoor, H. R. Bowman, and S. G. Thompson, *Phys. Rev.* **140**, B1310 (1965).

⁹ L. Bridwell, M. E. Wyman, and B. W. Wehring, *Phys. Rev.* **145**, 963 (1966).

¹⁰ C. D. Coryell (private communication).

¹¹ W. John (private communication).

All of the x-ray measurements satisfied either 1 or 2 but not both. The coincidence experiments used NaI(Tl) scintillators, proportional counters, or semiconductor detectors for the x-ray spectrometer.¹⁻⁹ The resolution was insufficient to make any prediction as to the relative population of adjacent elements. The experiments where high-resolving-power bent-crystal spectrometers (Cauchois type) were used were not coincidence experiments.^{10,11}

We decided to attempt the measurement of the coincident x-ray spectrum with a dispersive spectrometer capable of resolving adjacent- Z fission fragments. The coincidence requirement was satisfied by detecting one of the fission fragments in an ionization chamber. Only x rays which were in coincidence with the output pulse of the ionization chamber were accepted for energy analysis. The resolution requirement was not so easily satisfied. For simplicity of analysis, the K x rays whose series contains two prominent lines ($K\alpha$ and $K\beta$), were selected for analysis rather than the L x rays, whose series contains five prominent lines. The resolving power required to resolve $K\alpha$ x rays of adjacent- Z fission fragments is about two times larger than the resolving power available from proportional counters and about six times larger than the resolving power available from scintillation detectors. Therefore, a dispersive x-ray spectrometer of the Johansson type was chosen.

The requirements of high-resolving-power and high-detection sensitivity are mutually conflicting. That is, as the resolving power of a dispersive spectrometer is increased, the detection sensitivity is decreased. In order to have reasonable counting rates, a compromise value for the resolving power was selected. It was one which was high enough to resolve the $K\alpha$ x rays of adjacent- Z fission fragments. One would like to resolve each $K\alpha$ line from the closest $K\beta$ line (produced by a different element) or any γ lines present, but intensity requirements prohibit the high-resolving-power that would be required. Since the energy and the relative

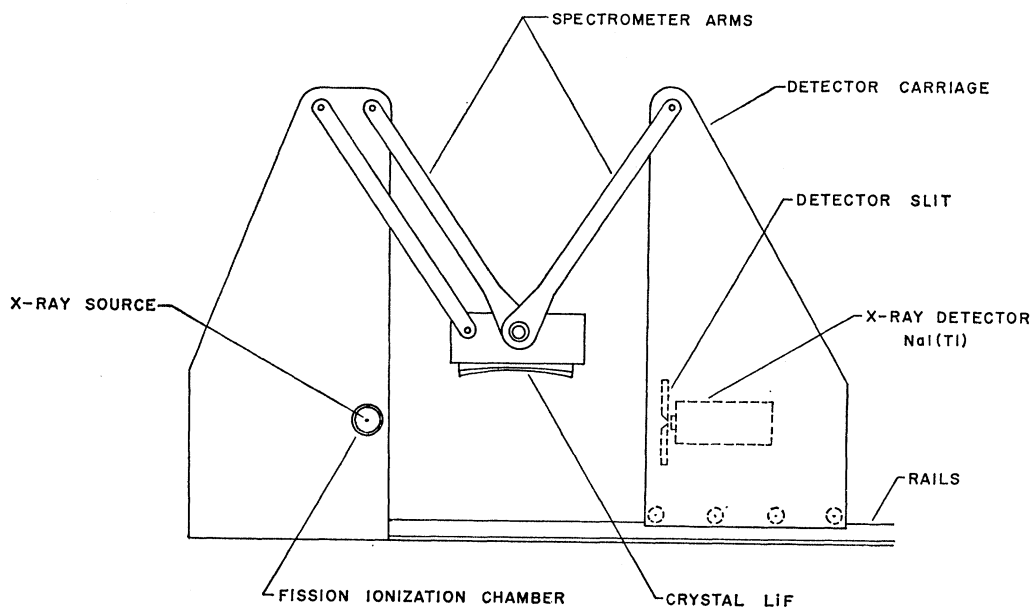


FIG. 1. Schematic drawing of the bent-crystal spectrometer used for the coincident x-ray measurements. The distance between pivots of the spectrometer arms is equal to the radius of the focal circle, 40 cm.

intensity of the $K\beta$ lines are known, their effect was calculated from the intensity of the corresponding $K\alpha$ lines. The number of γ 's coincident with fission in the K x-ray energy region was assumed to be small.¹⁰

Since the emission times reported by Bridwell *et al.*⁹ are comparable to the slowing down times for the fission fragments in the ionization chamber gas, Doppler broadening of the sharp lines was considered. If one assumes that all of the x rays are emitted when the fragments have their initial velocities, the sharp K x-ray lines are broadened to such an extent that they would overlap one another. Therefore, K x rays of adjacent Z 's could not be resolved regardless of the resolving power of the spectrometer. However, in this experiment all of the x rays are not emitted from a fission fragment moving with its initial velocity. One of the fragments leaves the foil and is detected while the other fragment stops in the foil. A considerable portion of the x rays emitted by the latter fragment experiences little Doppler shift in energy.

II. EXPERIMENTAL SYSTEM

A. Bent-Crystal Spectrometer

A bent-crystal spectrometer of the Johansson type was designed and constructed for the x-ray measurements. Figure 1 shows a schematic drawing of the spectrometer. X rays from the source strike the surface of the crystal and are focused to the detector slit by Bragg reflection. A shadow shield placed between the source and detector shielded the "straight-on" radiation. This energy-selective focusing required bending of the crystal and profiling of the surface. The reflective,

exact-focusing geometry was proposed by DuMond^{12,13} and used by Johansson.¹⁴

Because of its good reflection properties in the energy range of interest, lithium fluoride was chosen for the spectrometer crystal. The reflecting planes are the cleavage planes with $d=2.014 \text{ \AA}$.¹⁵ The radius of the focal circle is 40 cm. The crystal which was constructed by the Harshaw Chemical Company is made up of six single crystals of lithium fluoride. A number of flat crystals ($1\frac{1}{2}$ by $3\frac{1}{2}$ in.) were prepared by cleavage and then tested for singularity, intensity, and resolution. Six were chosen, individually bent, and bonded with epoxy onto a single aluminum backing plate ($4\frac{1}{2}$ by 7 in.). A vacuum technique was used to minimize the thickness of the layer of epoxy between the backing plate and crystals. The complete crystal assembly was then ground to the required radius.

The arm arrangement permits the source to remain fixed while keeping the spectrometer focused for all energy x rays. The Bragg angle is changed by moving the detector carriage horizontally along rails by means of a precision lead screw. The distance between the detector and the source (called D) gives the x-ray energy setting of the spectrometer. It is related to the Bragg angle by

$$D = 2R \sin 2\theta, \quad (1)$$

¹² J. W. M. DuMond and H. A. Kirkpatrick, *Rev. Sci. Instr.* **1**, 88 (1930).

¹³ J. W. M. DuMond, *Rev. Sci. Instr.* **18**, 626 (1947).

¹⁴ T. Johansson, *Z. Physik.* **82**, 507 (1933).

¹⁵ W. P. Amsbury, W. W. Lee, J. H. Rowan, and G. E. Walden, Atomic Energy Commission Report No. Y-1470-C, 1964 (unpublished).

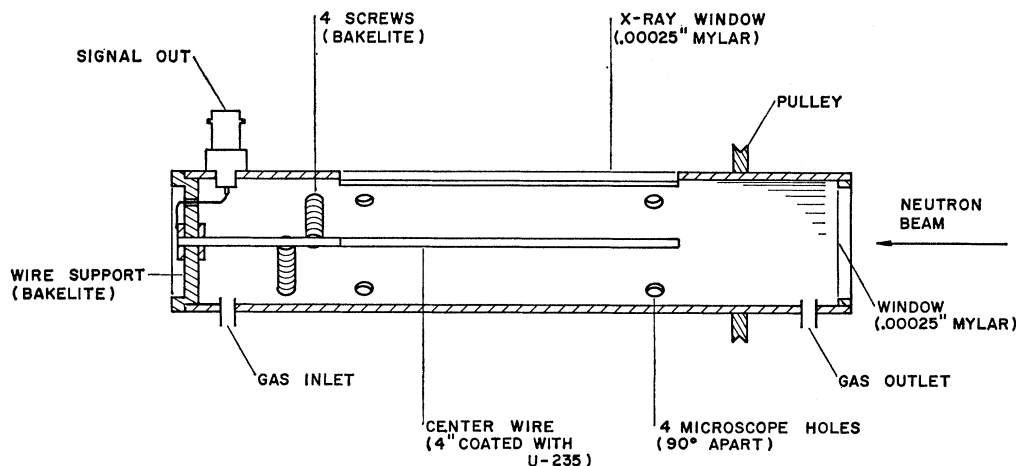


FIG. 2. Cross section of the cylindrical fission ionization chamber used for fragment detection. The coated wire served both as the x-ray spectrometer source and the center wire for the chamber.

where R is the radius of the focal circle and θ is the Bragg angle. D covers a distance range from 10 to 30 in., resulting in a range of energies from 5.2 to 19.2 keV for first-order reflections and 10.4 to 38.4 keV for second-order reflections.

The light-fragment x rays fall in the energy interval from 10 to 20 keV, while the heavy-fragment x rays fall between 20 and 40 keV. As the detector carriage is moved from $D=10$ to $D=20$ in. the crystal reflects the light-fragment x rays in first order and the heavy-fragment x rays in second order. By using an x-ray detector in the spectrometer which had sufficient resolution to separate first-order and second-order reflections, both the light-fragment x rays and the heavy-fragment x rays were counted at the same time.

B. Fission Source and Detection

The fission source was a 1-mm-diam beryllium wire coated with uranium enriched to 93% U^{235} to a thickness of 6 ± 2 mg/cm². It was fissioned in a neutron beam which emerged from the tangential beam port of the University of Illinois TRIGA Mark II Nuclear Reactor. The beam was confined by a specially constructed collimator which had a conical duct over most of its length. The diameter of the exit hole was $\frac{1}{2}$ in. Since it was not desirable to move the spectrometer away from the port between data collection runs, a shutter was provided for the collimator.

Figure 2 shows the cylindrical ionization chamber (diam=1.25 in.) used to detect fission events. It was free to rotate in polyethylene bushings in the spectrometer and could be removed and replaced easily. A unique feature was a belt-pulley system which rotated the chamber as the Bragg angle was changed. This was done in such a way that the same portion of the source always faced the center of the spectrometer crystal. The ionization chamber was a flow-type counter using methane. The coated wire served both as the x-ray

spectrometer source and the center wire for the chamber. The adjusting screws were used to adjust the position of the wire. This position was checked by looking with a microscope at the edge of the source wire. By noting the position of the wire with respect to a graduated scale and then rotating the ionization chamber 180° and again noting the position of the wire, the displacement of the wire from the center of the chamber was measured. With a thinly coated wire, the two kinetic-energy peaks of the fission fragments were clearly observed and separated from the α peak. By setting the

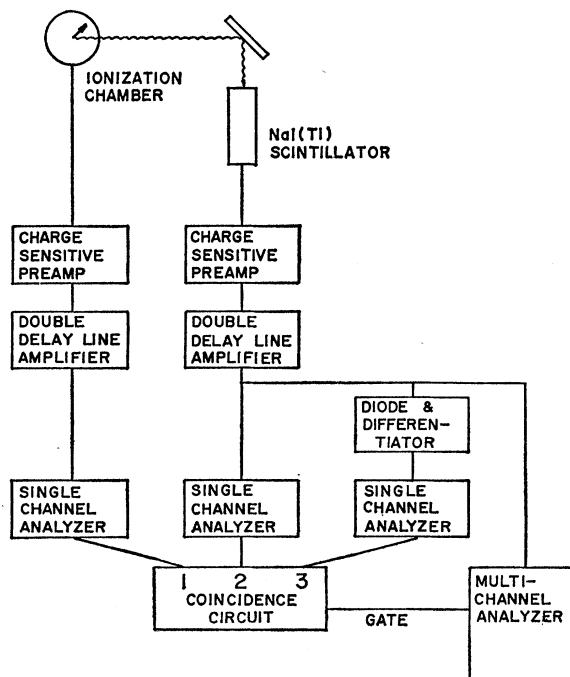


FIG. 3. Block diagram of the electronic equipment used for the coincident x-ray measurements.

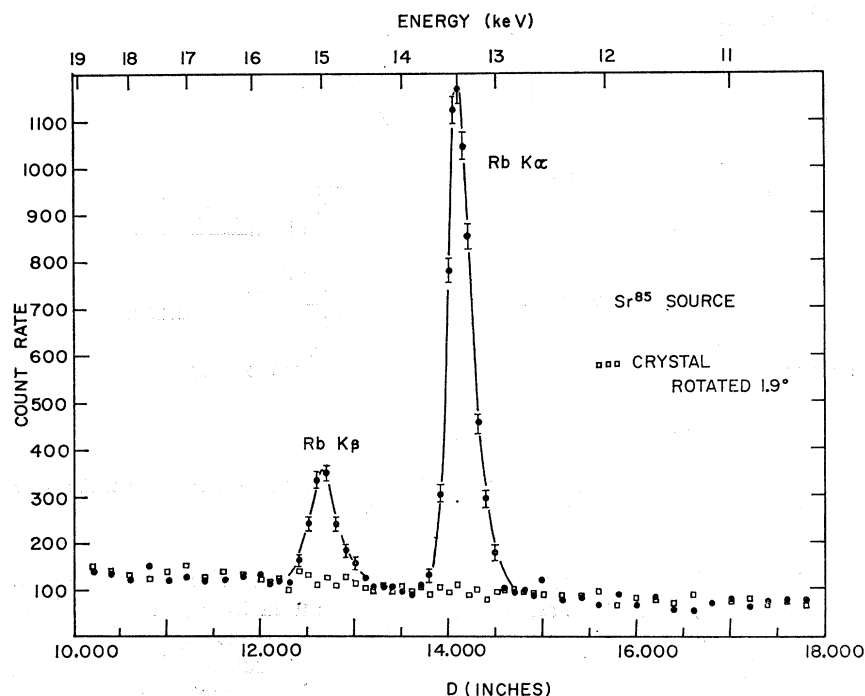


FIG. 4. First-order spectrum of the Sr^{85} calibration source as taken with the bent-crystal spectrometer. The variable D is the distance between the source and the detector and determines the energy setting of the spectrometer.

lower discriminator level above the α peak, only fission pulses were passed to the coincidence circuit.

C. X-Ray Detection

The spectrometer-detector slit was 10 cm long and 1 mm wide. The x-ray detector positioned behind this slit was a unit of two Harshaw Type 8 SH Integral Line detectors. Each included the following:

1. NaI(Tl) crystal (2 in. long by $\frac{1}{8}$ in. wide by 1 mm thick);
2. quartz light pipe (2-in. diameter by $\frac{1}{2}$ in. thick);
3. selected photomultiplier tube (2-in. diam);
4. beryllium window (2-in. diam by 0.005 in. thick).

Without the quartz light pipe it was experimentally determined that insufficient resolution could be maintained to separate first-order and second-order reflections. With the quartz light pipe sufficient resolution was obtained but it was found that a sizable portion of the background pulses had rise times which were not characteristic of x-ray scintillations in NaI(Tl). The rise time of these unexpected events was less than 0.10 μsec as compared to 0.25 μsec rise time for x-ray events. These events were attributed to high-energy scintillations¹⁶ and/or Čerenkov radiation¹⁷ in the quartz light pipe [the volume of the quartz was much larger than the volume of the NaI(Tl) crystal]. The elimination of these fast rise-time pulses by pulse-shape discrimination is described in the next section.

¹⁶ W. D. Compton (private communication).

¹⁷ J. Bellian (private communication).

D. Electronic Equipment

Figure 3 shows the schematic diagram of the electronic equipment used. The circuits of the first two coincidence channels (channels 1 and 2) are standard circuits. The single-channel analyzers selected the fission fragments and the x-ray energy range of interest. Double-delay-line shaping in the amplifiers permitted accurate coincidence timing ($2\tau \approx 0.10 \mu\text{sec}$) and high-fission count rates. The coincidence circuit gated the multichannel analyzer which recorded the coincidence NaI(Tl) spectrum.

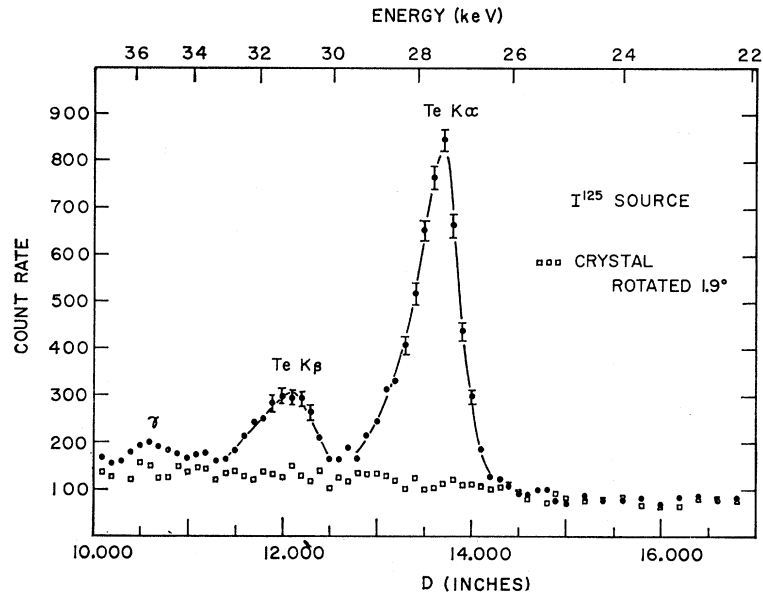
The purpose of the third channel was to eliminate the fast rise-time pulses described in the previous section. It utilized the fact that the baseline crossing time for a double-delay line-clipped pulse exhibits a dependence on rise time which is different than that shown by a RC clipped pulse. The discrimination was accomplished by comparing the baseline crossing time of the double-delay line pulse with the baseline crossing time of this pulse after it had been rectified and differentiated. The third channel was in anticoincidence with the other two channels and the delays were set to eliminate the fast events.

III. EXPERIMENTAL PROCEDURE

A. Spectrometer Calibration

Four radioactive sources Ge^{71} , Sr^{85} , Cd^{109} , and I^{125} were used for the calibration of the spectrometer. $K\alpha$ and $K\beta$ lines of the $Z-1$ daughter of each provided a total of eight energy references. The measurements

FIG. 5. Second-order spectrum of the I^{125} calibration source as taken with the bent-crystal spectrometer. The variable D is the distance between the source and the detector and determines the energy setting of the spectrometer.



were made over the entire range of D . Only the expected $K\alpha$ and $K\beta$ peaks were observed. After a spectrum was taken, the crystal was rotated 1.9° and the measurement was repeated. With the crystal rotated, no coherent reflection was observed in the range of D covered. The results of the Sr^{85} and I^{125} measurements are shown in Figs. 4 and 5, respectively.

The first-order calibration spectra all showed asymmetry with the larger tail on the right (large D). This asymmetry was experimentally found to be due to "cross-fire error." An x ray which is emitted from one end of the source and detected by the other end of the detector sees a slightly smaller Bragg angle than an x ray which is emitted from the center of the source and detected by the center of the detector. The second-order calibration spectra all showed asymmetry in the opposite direction (small D). This asymmetry was attributed to "penetration error." The higher-energy x rays penetrate some distance before they reflect off the crystal planes. Only the planes at the surface of the crystal satisfy the criteria for exact focusing.

Figure 6 shows the full width at half-maximum (FWHM) of the spectrometer for both first- and second-order spectra. The solid line is the FWHM calculated using $FWHM = E(\Delta\theta/\tan\theta)$, where $\Delta\theta$ is the angular uncertainty due to the source and slit width and θ is the Bragg angle. The cross-fire error appears to have little effect on resolving power while penetration error does substantially decrease the second-order resolving power. Figure 7 gives the measured efficiency of the spectrometer for first- and second-order spectra. Efficiency, as it is used here, is the peak counting rate divided by the total number of x rays emitted by the source per unit time. That is, with the spectrometer carriage set on the proper D for a monoenergetic x-ray source, about one x ray will be

detected for every 10^4 emitted. The solid lines are fitted to the experimental points.

B. Data Acquisition

The measurement of the intensity of x rays coincident with fission was made with a steady-state reactor power of 250 kW. About 7×10^4 fissions per second were detected. For each D setting of the spectrometer (energy value), a multichannel-analyzer spectrum was taken of the coincident NaI(Tl) detector output. The background was measured by rotating the crystal 1.9° and repeating the procedure. After subtracting the background spectrum, the count rates for the first-order and second-order energies corresponding to the D setting were found by adding the counts in the channels between appropriate limits. These limits were calculated using the Gaussian response shown by the NaI(Tl) scintillation detectors. In the energy region of interest, the energy response of the NaI(Tl) scintillation detectors was linear and the FWHM was proportional to the square root of the energy.

Because of poor signal-to-noise ratio, the background measurement had to be relatively accurate. By rotating the crystal 1.9° , while leaving everything else the same, only coherent reflections were eliminated from the NaI(Tl) spectra. The background, a portion of which is noncoherent scattering from the crystal, is not very sensitive to a 1.9° rotation of the crystal since the geometry for noncoherent scattering remains essentially the same.

At the start and end of each run, the shadow shield was removed from the spectrometer, the crystal was rotated 1.9° , the detector slit was removed, and a "straight-on" spectrum was taken. Figure 8 shows the result of one such "straight-on" spectrum. This pro-

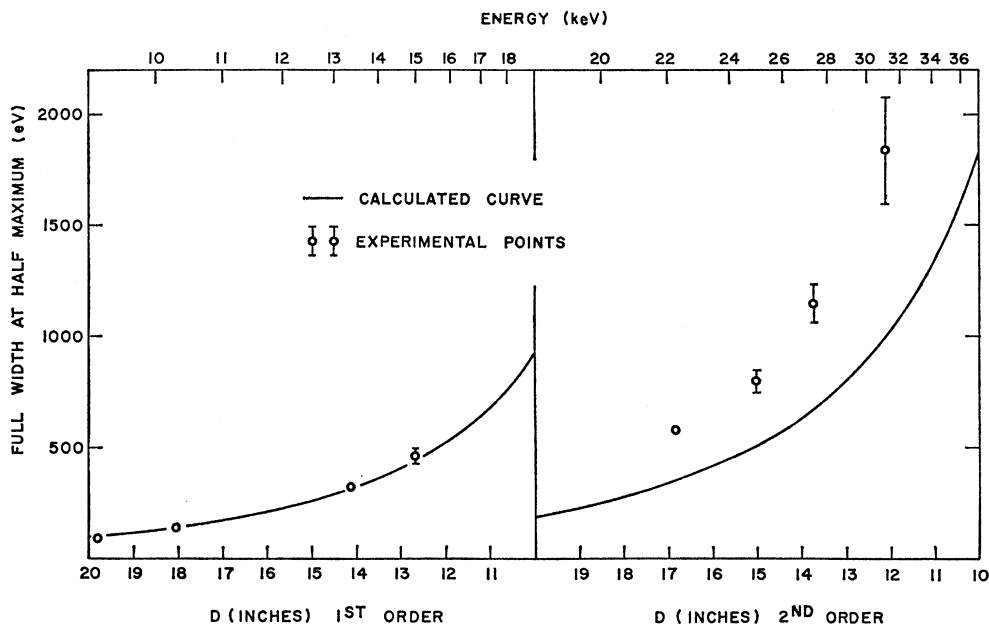


FIG. 6. Resolution of the bent-crystal spectrometer given as full width at half-maximum. The variable *D* is the distance between the source and the detector and gives the energy setting of the spectrometer.

cedure was followed in order to keep a "running check" on the system. These spectra can also be compared with previous fission x-ray measurements. Table I gives the number of x rays per fission calculated from the "straight-on" measurements. The results of other measurements are shown for comparison.

C. Data Analysis

The experimental data were analyzed by the method of least squares. The shape of the peak for each x-ray line was predicted from the measured response of the spectrometer. Intensities of the x rays were then calculated by fitting the experimental data by the

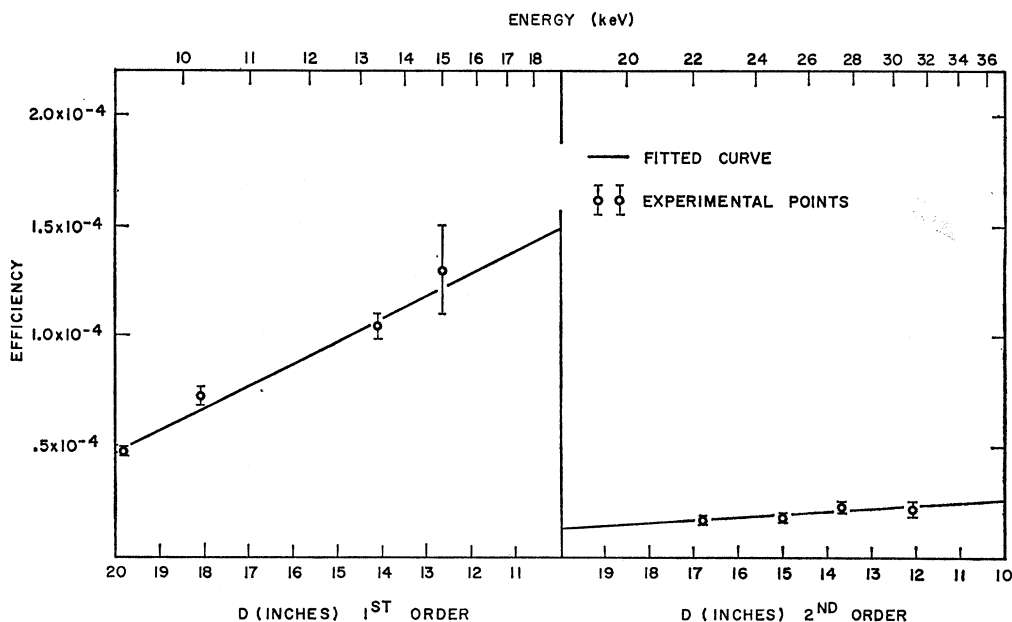


FIG. 7. Efficiency of the bent-crystal spectrometer expressed as peak counting rate divided by total source emission rate. The variable *D* is the distance between the source and the detector and determines the energy setting of the spectrometer.

FIG. 8. "Straight-on" fission x-ray spectrum taken by removing the shadow shield from the spectrometer, rotating the crystal, and removing the detector slit from in front of the NaI(Tl) scintillators.

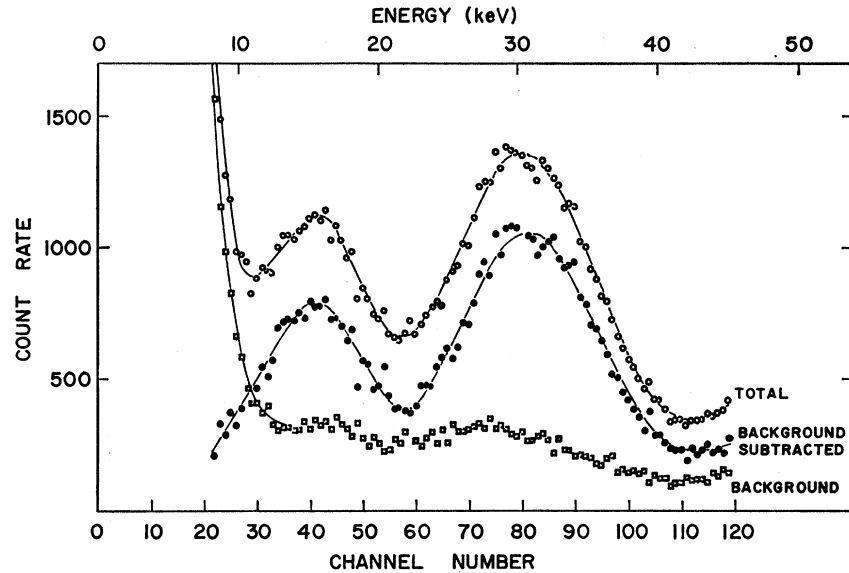


TABLE I. The light- and heavy-fragment x-ray yields for thermal-neutron fission of U^{235} .

Light-fragment yield (x rays/fission)	Heavy-fragment yield (x rays/fission)	Reference
0.12 ± 0.03	0.20 ± 0.05	"Straight-on" spectrum (this work)
0.10 ± 0.03	0.42 ± 0.12	3
0.08^a	0.12^a	5
0.17 ± 0.02	0.43 ± 0.04	9

^a Reference 5 gives the results for the sum of both the heavy- and light-group x rays as 0.20 x rays/fission. Hohmann's data suggest this as a reasonable division.

following function:

$$C(D) = \sum_i \sum_j A_i G_{ij} \phi(D, D_{ij}), \quad (2)$$

where A_i is the intensity of the $K\alpha$ x ray from the i th element, G_{ij} is the relative intensity of the j th line of the i th element ($G_{iK\alpha} = 1$), ϕ is the normalized fission x-ray peak shape, and D_{ij} is the D setting corresponding to the energy of the j th line of the i th element. The $G_{iK\beta}$ values are known both from previous measurements¹⁸ and from the calibration spectra measurements.

Two effects made the fission x-ray peaks broader than the peaks measured using the calibration sources. The first effect is Doppler broadening of the lines, because some of the x rays are emitted from moving fission fragments. The second effect is caused by x rays that are emitted by fragments which have traveled some distance away from the source wire and hence are

slightly out of focus. If the fragments are too far from the source wire, however, the x rays will not be counted at all. The exact effect on the shape of the fission x-ray peaks due to these two factors is difficult to calculate.

The procedure which was followed approximated the fission x-ray peaks by the sum of a non-Doppler-broadened component plus a fully Doppler-broadened component. If f is the fraction of x rays in the fully Doppler-broadened component, a fission x-ray peak at D_0 can be described by

$$\phi(D, D_0) = (1-f)R(D, D_0) + f\psi(D, D_0), \quad (3)$$

where $R(D, D_0)$ is the response of the spectrometer to a monoenergetic x-ray line at D_0 and $\psi(D, D_0)$ is the response of the spectrometer to a fully Doppler-broadened line at D_0 . The least-squares calculations were made using different values of f . The reasoning behind this procedure is that Eq. (3) is not necessarily meant to represent the physical process, but to give a good approximate shape for the fission x-ray peaks. The f which gave the minimum χ^2 , the range of f values which gave reasonable fits according to a χ^2 criterion, and the dependence on f of the calculated intensities were found. The standard deviations of the A_i values were estimated by the method described by Hildebrand.¹⁹

The functional form of $R(D, D_0)$ was found by trial and error fitting of various analytic shapes to the calibration data. A skewed Gaussian of the following form gave the best fit:

$$R(D, D_0) = \exp[-0.6932(D - D_0)^2/\Gamma^2] \\ = \exp[-0.6932(D - D_0)^2/\Gamma^2] + B(D - D_0)^2 \exp[-0.6932(D - D_0)^2/\Gamma'^2],$$

$D \leq D_0$ first order,
 $D \geq D_0$ second order;
 $D > D_0$ first order,
 $D < D_0$ second order.

¹⁸ A. H. Compton and S. K. Allison, *X-Rays in Theory and Experiment* (D. Van Nostrand Company, Inc., New York, 1957).

¹⁹ F. B. Hildebrand, *Introduction to Numerical Analysis* (McGraw-Hill Book Company, Inc., New York, 1956).

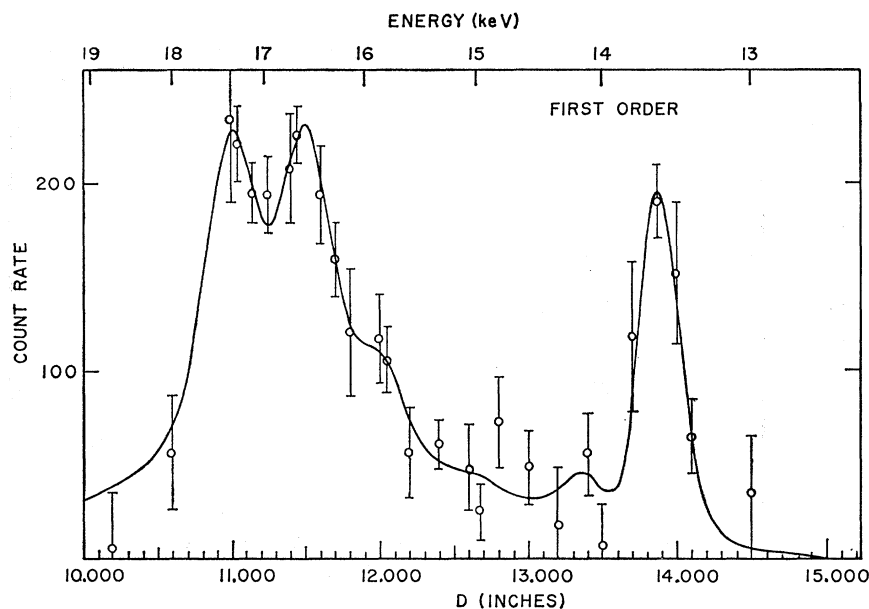


FIG. 9. First-order spectrum of x rays coincident with fission of U^{235} as taken with the bent-crystal spectrometer. The variable D is the distance between the source and the detector and determines the energy setting of the spectrometer.

The dependence of D_0 on x-ray energy was that given by Eq. (1) with a small linear correction. The dependence of Γ and Γ' was calculated from the resolving power, while the dependence of B was completely empirical. The Bragg angle for the calibration x-ray energies was taken from tables compiled by Amsbury *et al.*¹⁵ The function $R(D, D_0)$ fitted all calibration spectra within experimental statistical error. The response of the spectrometer to a Doppler-broadened line at D_0 is then given approximately by

$$\psi(D, D_0) = [2(v/c)D_0(1 - \tan^2\theta_0)]^{-1} \times \int_{-(v/c)D_0(1 - \tan^2\theta_0)}^{(v/c)D_0(1 - \tan^2\theta_0)} R(D, D') dD',$$

where v is the initial velocity of the fragment corresponding to D_0 , c is the velocity of light, θ_0 is the Bragg angle, and $R(D, D')$ is the monoenergetic response of the spectrometer. The initial velocities of the fragments were calculated from the data of Stein²⁰ using the relationship given by Wahl²¹ which relates the most probable charge to fragment mass.

IV. RESULTS

The results of the fission x-ray measurement for the first-order spectrum are shown in Fig. 9. The solid curve is the result of fitting Eq. (2) to the experimental points. Doppler-broadened $K\alpha$ and $K\beta$ peaks of ^{87}Rb , ^{88}Sr , ^{89}Y , ^{90}Zr , ^{91}Nb , and ^{92}Mo as well as the non-broadened L x-ray peaks of uranium were used for the fitting calculation. The $L\alpha_1$ line of uranium falls between

two K peaks of the fragments. The other less intense L lines of uranium fall more or less on top of K lines of the fission fragments and their intensities were determined from the intensity of the $L\alpha_1$ line. For this experiment, the uranium L x rays represented about 25% of the light-fragment peak and are believed to be due to the photoelectric effect of the heavy-fragment x rays in the relatively thick uranium foil. The value of f which gave the minimum χ^2 was 0.7 and the results obtained from that calculation are reported. The range of f values which gave reasonable fits was 0.4 to 1.0. The shape of the resulting curve was sensitive to the value of f used for the calculation but the values of the intensities of the $K\alpha$ x rays were rather insensitive to this quantity. The variation of the calculated intensities for a reasonable range of f (0.5 to 0.8) was less than one standard deviation. Figure 10 shows the individual contributions of the K x-ray peaks to the first-order spectrum.

The results for the second-order spectrum were inconclusive because of the lower resolving power and lower efficiency of the spectrometer for the heavy-fragment x rays as compared to the light-fragment x rays. The calculated standard deviations for the intensities of the $K\alpha$ x rays of the different heavy elements were approximately equal to the magnitude of the largest intensity.

Figure 11 gives the number of K x rays per fission emitted by the various elements. The intensities, counting both $K\alpha$ and $K\beta$ for any element, were calculated by the least-squares program and divided by the fission rate. They were corrected for spectrometer efficiency and absorption in the uranium. Both light-fragment and heavy-fragment results are shown for completeness. However, the relative x-ray yields of

²⁰ W. E. Stein, Phys. Rev. **108**, 94 (1957).

²¹ A. C. Wahl, R. L. Ferguson, D. R. Nethaway, D. E. Troutner, and K. Wolfsberg, Phys. Rev. **126**, 1112 (1962).

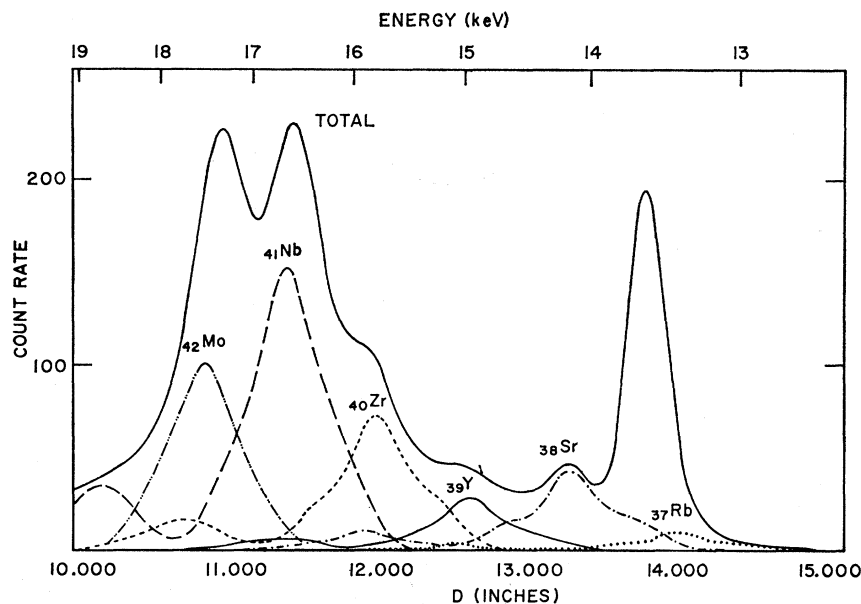


FIG. 10. Individual contributions of the fragment K x-ray peaks to the first-order spectrum of the x-rays coincident with fission of U^{235} . Additional L x-rays from uranium occur in the spectrum such as the $L\alpha_1$ line at 13.6 keV, $L\beta_1$ line at 17.2 keV, and the $L\beta_2$ at 16.4 keV.

adjacent heavy fragments have little significance due to the large standard deviations involved. The gross features of the heavy-fragments yields do agree qualitatively with previous measurements. These results are compared to the initial yields calculated by Ferguson and Read.²² Their method correlated the available mass, energy, and yield data in order to make a prediction.

The apparent variation of x-ray yield per element can be explained by assuming the dominant mechanism for the production of K vacancies is internal conversion

by the de-exciting fragments. The energy-level spacing for nuclei in the region of closed shells (spherical nuclei) tends to be large and, therefore, internal conversion de-excitation less probable. Moving away from the closed-shell regions, one expects to find deformed nuclei. They give rise to transitions of lower energies, which have a larger probability of internal conversion and also longer lifetimes. Timing measurements of the x-ray emission with respect to the fission event are consistent with these assumptions.⁹ Figure 12 shows the nuclide

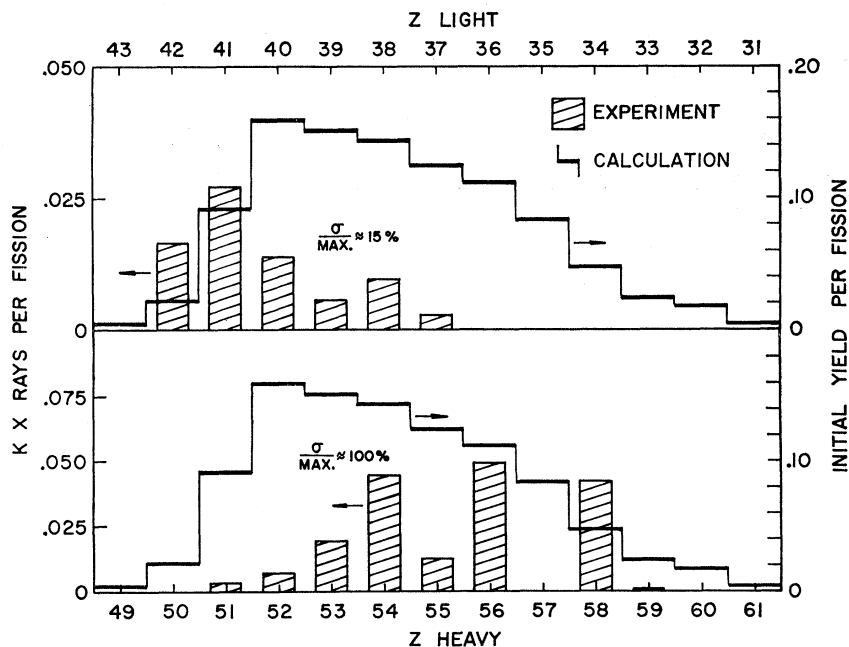


FIG. 11. Number of K x-rays per fission as determined by the coincident x-ray measurements. The relative x-ray yields of adjacent heavy fragments have little significance due to the large standard deviations involved, but the gross features agree qualitatively with previous measurements. The results of the initial fragment yield calculations of Ferguson and Read are given for comparison. (See Ref. 22.)

²² J. M. Ferguson and P. A. Read, Phys. Rev. 139, B56 (1965).

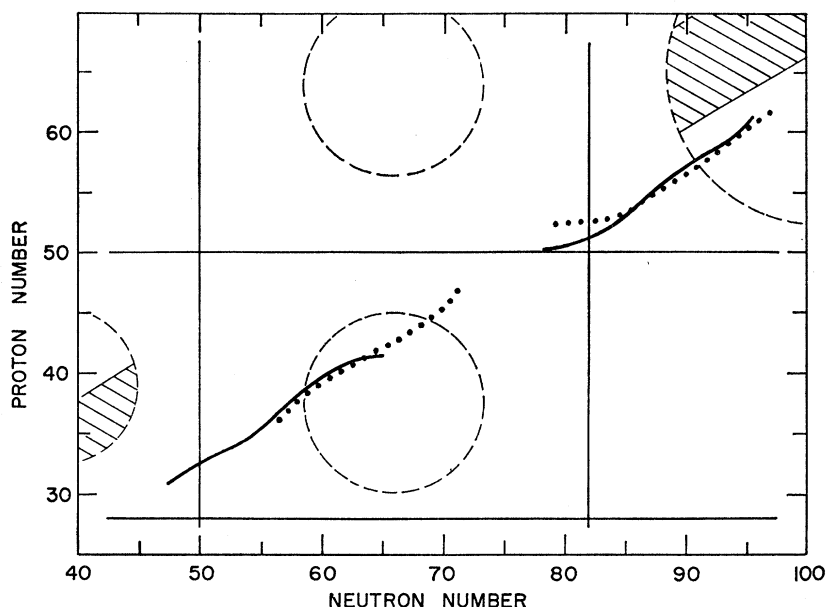


FIG. 12. The portion of the Z -versus- N chart showing the nuclide region of interest. The straight lines locate neutron and proton closed shells. The heavy solid curves indicate the most probable initial fission fragments of U^{235} . The heavy dotted curves indicate the most probable initial fission fragments of Cf^{252} . Regions where deformed nuclei might be found are shown by dashed circles. The shaded areas inside the dashed circles show two groups of nuclides having rotational spectra of the type predicted for deformed nuclei.

region of interest and locates the closed nuclear shells at 28, 50, and 82. The heavy solid curves indicate, from available measurements, the most probable initial fission fragments of U^{235} .²¹ Regions where deformed nuclei might be found are indicated by dashed circles.²³ Two groups of nuclides having rotational spectra of the type predicted for deformed nuclei are indicated by shading.²³ The nuclear charges for the fission fragments which fall in the deformed-nuclei regions are the ones which were observed to emit most of the K x rays. This agreement may be taken as experimental evidence for the existence of these deformed-nuclei regions. Also shown in Fig. 12 as dotted curves is the most probable initial fission fragments of Cf^{252} .⁷ In this case the light-fragment yield occurs in the deformed-nuclei region. Hence, most of the light fragments should emit x rays.

²³ E. Segrè, *Nuclei and Particles* (W. A. Benjamin, Inc., New York, 1964).

This is consistent with the x-ray measurements of Glendenin *et al.*⁷ and Kapoor *et al.*⁸ In the case of thermal-neutron induced fission of U^{235} the expected yield of light fragments is only partly in the deformed-nuclei region. This would produce a strong emphasis in the x-ray yield for that region, as is seen in the data.

ACKNOWLEDGMENTS

The authors are indebted to many people for their assistance in various aspects of this work: Dr. L. B. Bridwell for many helpful discussions of the experimental and computational problems; The Harshaw Chemical Company for the construction of the LiF monochromator; the University of Illinois Physics shop for the construction of the bent-crystal spectrometer; P. R. Hesselmann for his help in the preparation of the radioactive sources; G. P. Beck and S. E. Boudreaux for operation of the reactor.